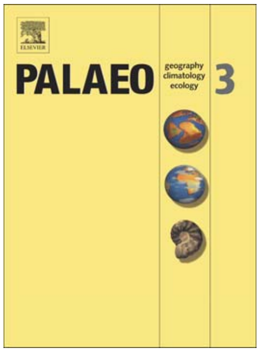

Late glacial to Holocene climate change and human impact in the Mediterranean: the last ca. 17 ka diatom record of Lake Prespa (Macedonia/Albania/Greece)

Aleksandra Cvetkoska, Zlatko Levkov, Jane M. Reed, Bernd Wagner

PII: S0031-0182(14)00193-X
DOI: doi: 10.1016/j.palaeo.2014.04.010
Reference: PALAEO 6832

To appear in: *Palaeogeography, Palaeoclimatology, Palaeoecology*

Received date: 22 October 2013
Revised date: 5 April 2014
Accepted date: 8 April 2014

Please cite this article as: Cvetkoska, Aleksandra, Levkov, Zlatko, Reed, Jane M., Wagner, Bernd, Late glacial to Holocene climate change and human impact in the Mediterranean: the last ca. 17 ka diatom record of Lake Prespa (Macedonia/Albania/Greece), *Palaeogeography, Palaeoclimatology, Palaeoecology* (2014), doi: 10.1016/j.palaeo.2014.04.010

Late glacial to Holocene climate change and human impact in the Mediterranean: the last ca. 17 ka diatom record of Lake Prespa (Macedonia/Albania/Greece)

Aleksandra Cvetkoska[1], Zlatko Levkov[1], Jane M. Reed[2] & Bernd Wagner[3]

[1]Institute of Biology, Faculty of Natural Sciences, Ss Cyril and Methodius University, Skopje, R. Macedonia

[2]Department of Geography, Environment and Earth Sciences, University of Hull, Hull, UK

[3]Institute of Geology and Mineralogy, University of Cologne, Cologne, Germany

Corresponding author:

Aleksandra Cvetkoska

Institute of Biology, Faculty of Natural Sciences

Arhimedova 3, 1 000 Skopje

Macedonia

Tel: ++ 389/2/3249-601

e-mail: acvetkoska@yahoo.com

Abstract

Lake Prespa (Macedonia/Albania/Greece) occupies an important location between Mediterranean and central European climate zones. Although previous multi-proxy research on the Late Glacial to Holocene sequence, core Co1215 (320cm; ca. 17 cal ka BP to present), has demonstrated its great value as an archive of Quaternary palaeoclimate data, some uncertainty remains in the interpretation of climate change. With the exception of oxygen stable isotope data, previous palaeolimnological interpretation has relied largely on proxies for productivity. Here, existing interpretation is strengthened by the addition of diatom data. Results demonstrate that shifts in diatom assemblages composition are driven primarily by lake-level changes and thus permit more confident interpretation of shifts in moisture availability over time, while corroborating previous interpretation of catchment- and climate-induced productivity shifts. An inferred cold, arid shallow lake phase between ca. 17.1–15.7 cal ka BP is followed by a high-productivity phase from ca. 15.7 cal ka BP with Late Glacial warming, but also the first evidence for a gradual increase in lake level, in line with other regional records. Clear evidence for a Younger Dryas climate reversal between ca. 13.1–12.3 cal ka BP is followed by an unusually gradual transition to the Holocene and deeper, oligotrophic-mesotrophic lake conditions are reached by ca. 11.0 cal ka BP. In contrast to the arid episode from ca. 10.0–8.0 ka inferred from positive $^{18}\delta O_{calcite}$ values, rapid diatom-inferred lake-level increase after the start of the Holocene suggests high moisture availability, in line with palynological evidence, but with only very subtle evidence for the impact of an 8.2 ka cold event. The maintenance of high lake levels until 1.9 cal ka BP, and the peak of inferred humidity from ca. 7.9–6.0 cal ka BP, matches the oxygen stable isotope profile and confirms that the latter is driven primarily by evaporative concentration rather than reflecting regional shifts in precipitation sources over time. During the Late Holocene progressive eutrophication is inferred between 1.9 – present.

Two shallow phases at ca. 1.0 cal ka BP and at ca. 100 years ago probably represent an aridity response which is added to increased human impact in the catchment. Overall, the study is important in confirming previous tentative inferences that Late Glacial to Holocene moisture availability has strong affinity with other sites in the Eastern Mediterranean. It also tracks the pattern of North Atlantic forcing.

Key words: Lake Prespa; diatoms; lake level; productivity; Mediterranean; palaeoclimate.

1. Introduction

The Mediterranean is a region of high climatic spatial variability. Although Late Quaternary palaeoclimate data have improved substantially over the last decade (e.g. González-Sampériz et al. 2006, Kotthoff et al. 2011, Fletcher & Zielhofer 2013), we still require improved understanding of spatial variability in climate over time in order to understand the underlying climatic mechanisms (Tzedakis 2007). A prime example is the ongoing debate concerning the spatial distribution of moisture availability during the Holocene (Magny et al. 2012).

Balkan Lake Prespa is an ancient tectonic lake which probably formed > 2 Ma ago and is hydrologically connected through the mountain range Galicica with Lake Ohrid (Stankovic, 1960). Both lakes are renowned for their extraordinary biodiversity and high endemism (Albrecht & Wilke 2008). They are also located at an important junction between Mediterranean and continental European climate zones (Hollis & Stevenson 1997, Wagner et al. 2008). While Lake Ohrid is deep and oligotrophic, significant water level oscillations occur naturally in Lake Prespa (Sibinovic 1987), offering contrasting potential for palaeolimnological climate reconstruction.

Previous multi-proxy research on the Late Glacial to Holocene sequence of core Co1215 (320cm; ca. 17 cal ka BP to present) has focused largely on productivity indicators, linked to palynological evidence for catchment changes (Aufgebauer et al. 2012; Panagiotopoulos et al. 2013), with palaeohydrological data confined to oxygen stable isotope analysis (Leng et al. 2010, 2013). Although these studies demonstrate the great value of Lake Prespa as an archive of Quaternary palaeoclimate data, the interpretation of climate change is still uncertain. Diatoms (single-celled algae; Bacillariophyceae) are abundant, diverse and sensitive to a wide range of limnological variables, and can provide strong proxy evidence both for productivity and lake-level changes. Here, existing interpretation of Late Glacial to Holocene climate change in Lake Prespa is strengthened by the addition of diatom data, to address a key area of uncertainty in Mediterranean palaeoclimate reconstruction.

2. The study area

Lake Prespa (40° 46’–41° 00’ N, 20° 54’–21° 07’ E, or Macro Prespa, Fig. 1) is located in the Western–Macedonian geotectonic zone of the Dinarides at an altitude of 849 m a.s.l. The transboundary catchment (Macedonia, Albania and Greece) also contains the smaller lake, Micri Prespa. The two were formerly joined as a single lake basin; in 1969/1970, an artificial dam was constructed between the lakes to manage the water level of Lake Micro Prespa (Hollis & Stevenson, 1997). Both lakes are part of a former lake complex called the Dessarets (Stankovic, 1960), which includes Lake Ohrid and Lake Maliq (Korca basin). According to Radoman (1985) these tectonic basins are Tethys derivates formed during Alpine orogeny in the Late Tertiary. Cvijic (1911) suggested that the Dessarets have belonged to an Adriatic group of lakes which is isolated from the Aegean limnetic group. However, Bourcart (1922) suggested that there may have been some hydrological connection through the Korca depression and the Transaegean valley.

Lake Prespa currently has a surface area of 254 km^2, mean water depth of ca. 14 m, maximum water depth of ca. 48 m and a total volume of 3.6 km^3. The estimated hydraulic residence time is ca.11 years. The water balance is controlled by the input/output ratio. The water input depends on surface input from river inflow, catchment runoff, direct precipitation, Lake Micro Prespa inflow and groundwater input (no data available for the latter). The output is via surface evaporation, water abstraction for irrigation and subsurface outflow through the karstic aquifers of Galicica Mountain into Lake Ohrid (Matzinger et al. 2006). The climate may be described as Mediterranean in the southern and continental in the northern part of the catchment area, with sub–alpine character below 1650 m altitude and alpine character above this altitude. Annual temperature fluctuates from 1°C in winter to 21°C in summer, and annual precipitation varies between 720 and 1200 mm yr^{-1} in the lake's valley and the surrounding mountain ranges, respectively (Hollis & Stevenson, 1997). Major recent lake level fluctuations have occurred, with a decline of almost 10 m in between 1950 and 2009. The location of historical settlements and palaeo-shorelines around the lake indicates that Lake Prespa also experienced major lake-level fluctuations in the past (Sibinovic 1987). Recent accelerated anthropogenic eutrophication has occurred, with an increase in total phosphorus (TP) input from an historic mean of ca. 20 to 31 mg P m^{-3} in 2003 (Matzinger et al. 2006).

3. Material and methods

3. 1. Core recovery and chronology

The sediment core Co1215 was recovered in autumn 2009 at a water depth of 14 m in the central northern part of Lake Prespa (Wagner et al. 2012) from a floating platform equipped with gravity and piston corers (UWITEC Corp. Austria). Correlation of gravity and up to 3 m long piston core sections resulted in a 1575 cm long composite sequence with estimated age of ca. 91 cal ka BP. The age model of the sequence is based on tephrochronology, radiocarbon dating, electron spin resonance (ESR), accelerator mass spectrometry (AMS) and correlation with NGRIP ice core record and is described in more detail in Damaschke et al. (2013).

The uppermost 320 cm of core Co1215, used for this study, represents the Late Glacial-Holocene period or the last ca. 17 cal ka BP. The chronology of this part of the sequence is based on radiocarbon dating and tephrostratigraphy. Fourteen radiocarbon dates were obtained from accelerator mass spectrometry (AMS) and $\delta^{13}C$ analysis of selected plant macrofossils, fish bones, shell remains and bulk sediment samples (Table 1). The AMS measurements were performed at the ETH Laboratory in Zurich, Switzerland and the results are presented and discussed in more detail in Aufgebauer at al. (2012). The chronology was verified by identification of four tephra layers from well-dated Italian volcanic eruptions. These tephra layers are marked as PT0915–1 (55.4–55.6 cm depth), PT0915–2 (155.6–156.2), PT0915–3 (265–267 cm depth), PT0915–4 (287–289 cm depth) and the details of their geochemical composition and correlation with volcanic events are presented in Aufgebauer et al. (2012). The final age-depth model (Fig. 2) was established based on linear interpolation between the chronological tie points. All ages presented in this paper are calibrated to calendar ages (cal ka BP) with 2σ range.

3. 2. Diatom analysis

For the diatom analysis, ca. 0.1 g wet sediment subsamples were taken from the upper 320 cm of Lake Prespa core Co1215 at ca. 8 cm intervals (ca. 0.1 - 0.4 ka) and stored in Sterilin tubes at 4°C. Samples were cleaned using a modification of Renberg’s method for handling a large number of samples (Renberg 1990). Each sample was treated with cold H_2O_2 to oxidize organics and 10% HCl to remove carbonates. Diatom slides were prepared using Naphrax® as a mountant. Diatom assemblages were counted under oil immersion at x 1500 magnification with a Nikon Eclipse 80i microscope, and diatom images produced using a Nikon Coolpix P6000 camera. Approximately 400 diatom valves were counted per slide using the standard transect–based method (Battarbee 1986). Diatom taxa were identified using standard texts (Krammer and Lange-Bertalot, 1986, 1991a, b, 1997, 2000), and the dedicated Ohrid and Prespa taxonomic work of Levkov et al. (2007). Håkansson et al. (1990, 2002), Kiss et al. (1996, 1999) and Houk et al. (2010) were used for identification of the *Cyclotella ocellata* complex. Counts were converted to percentage data and summary data were displayed using Tilia and TGView v. 2.0.2. (Grimm 1991). Zone boundaries were defined with Constrained Incremental Sum of Squares cluster analysis (Grimm 1987). Multi-proxy stratigraphic diagrams were prepared using C2 (Juggins 1991-2007). Correlation between diatom taxa and geochemical proxies was tested using the Spearman's rho correlation test, in the statistical package “stats”, version 0.8-2 (R Core Team 2012). Variation in the diatom data was explored further by ordination. With a gradient length of >2.5, detrended correspondence analysis (‘DCA’) was appropriate (Jongman et al. 1995). DCA was performed using “vegan” version 2.0-4 (R Core Team 2012).

4. Results

4.1. Diatom proxies

A total of 187 diatom taxa was identified. Planktonic taxa from the genera *Cyclotella* and *Stephanodiscus* were dominant apart from at the base of the sequence. Small Fragilariales were highly diverse throughout the record. Benthic taxa including the genera *Campylodiscus*, *Navicula*, *Diploneis* and *Surirella* were present at low abundance. The summary diagram (Fig. 3) shows 35 diatom taxa present at > 2% relative abundance, some of which comprise groups of species. Five major assemblage zones (Prespa Diatom Zones PDZ 1–5) can be recognized from CONISS. Diatom data are compared to selected geochemical and pollen data from core Co1215 in Fig. 4.

4.2.1. Diatom assemblage zone PDZ 1 (321–293 cm depth, ca. 17.0 –15.7 cal ka BP)

The base of the sequence is dominated by facultative planktonic taxa. *Staurosirella pinnata* (Ehrenberg) Williams & Round is present at 40–60% throughout, reaching maximum relative abundance at the upper zone boundary. A wide range of benthic taxa are present at low abundance, decreasing from 30% at the base to 20 % at the upper zone boundary. *Campylodiscus marginatus* Jurilj, *Diploneis alpina* Meister, *Karayevia clevei* (Grunow) Bukhtiyarova, *Gyrosygma macedonicum* Levkov, Krstic & Nakov and *Surirella* spp. Turpin are common, reaching a relative abundance of ca. 10–16 % throughout.

4.2.2. Diatom assemblage zone PDZ 2 (293–236 cm depth, ca. 15.7–13.1 cal ka BP)

PDZ 2 marks a transition towards increased abundance of planktonic *Cyclotella* taxa at the expense of small Fragilariales, which occur at <20% in most of the zone. *Cyclotella ocellata* Pantocsek and *C. paraocellata* Cvetkoska, Hamilton, Ognjanova-Rumenova & Levkov are dominant; *C. minuscula* (Jurilj) Cvetkoska, characteristed by its small valves (3–7 µm diameter) and the endemic planktonic *C. prespanensis* Cvetkoska, Hamilton, Ognjanova-Rumenova & Levkov (Cvetkoska et al. in press) are also present; the latter attains a maximum of ca. 20% in the upper zone. *Stephanodiscus rotula* (Kützing) Hendey is also present at low abundance apart from a minor peak of ca. 9 % at 281 cm depth (ca. 15.2 cal ka BP) which is followed by an increase in *S. pinnata*. Benthic taxa are diverse and include *G. macedonicum*, *Surirella* spp., *Amphora* spp. Ehrenberg ex Kützing and *Diploneis mauleri* (Brun) Cleve. The small benthic species *N. submuralis* Hustedt is most abundant, reaching 5 % at 281 cm depth or ca. 15.2 cal ka BP.

4.2.3. Diatom assemblage zone PDZ 3 (236–220 cm depth, ca. 13.1–12.3 cal ka BP)

PDZ 3, although comprising only two samples, is clearly separated by the distinct peak in *Aulacoseira granulata* (Ehrenberg) Simonsen, reaching a maximum of 30% relative abundance at ca. 12.9 cal ka BP, followed by a short-lived return to dominance by *S. pinnata* at the upper zone boundary. The groups of *Cyclotella* and benthic taxa are present at low relative abundance of up to 30 % and 25 %, respectively.

4.2.4. Diatom assemblage zone PDZ 4 (220–70 cm depth, ca. 12.3–1.9 cal ka BP)

PDZ4 is divided in four subzones, PDZ 4a–PDZ 4d.

PDZ 4a (220–204 cm depth, ca. 12.3–11.5 cal ka BP) shows renewed plankton dominance. *Stephanodiscus rotula* is abundant (ca. 30%) at the base of the zone and declines thereafter as *C. paraocellata* increases to ca. 30%. *Aulacoseira granulata* and small Fragilariaceae are rare compared to PDZ3.

PDZ 4b (204–164 cm depth, ca. 11.5–9.3 cal ka BP) is dominated to >80% by planktonic taxa. *Cyclotella ocellata* and *C. paraocellata* are accompanied by *S. rotula*, which gradually declines to ca. 10% abundance at the upper zone boundary. *Cyclotella prespanensis, A. granulata* and small Fragilariales are rare, as well as the benthic species *Amphora* spp., *C. marginatus, C. striatus* Jurilj, *D. mauleri*, *G. macedonicum, Surirella* spp., *Eolimna rotunda* (Hustedt) Lange-Bertalot, Kulikovskiy & Witkowski and *Navicula hasta* Pantocsek.

A lower abundance of *S. rotula* and a higher proportion of the *C. ocellata–C. paraocellata* group delineate PDZ 4c (164–133 cm depth, ca. 9.3–7.9 cal ka BP). Facultative planktonic and benthic species are present at <20%. *Cyclotella minuscula* peaks in a single sample (ca. 10%) at ca. 8.0 cal ka BP, and is followed by the appearance of another small planktonic taxon, *Stephanodiscus* cf. *vestibulis* Håkansson, Theriot & Stoermer.

PDZ 4d (133–70 cm depth, ca. 7.9–1.9 cal ka BP) exhibits the maximum plankton dominance of the sequence, peaking at 95 % in the mid zone (ca. 6.0 cal ka BP). *Cyclotella paraocellata* is the most dominant, followed by *C. ocellata, C. prespanensis* and *S. rotula*. Benthic taxa and small Fragilariaceae are rare.

4.2.5. Diatom assemblage zone PDZ 5 (70–2 cm depth, ca. 1.9 cal ka BP–present)

PDZ 5 marks a transition towards the dominance of *C. ocellata* over *C. paraocellata* and *C. prespanensis*. It is a zone of major fluctuation compared to previous zones. The lowermost horizon is indicated by the renewed high abundance of *C. minuscula* (> 20%) at ca. 1.7 and 1.5 cal ka BP, followed by a decrease in the relative proportion of *C. ocellata*. A short-lived decrease in planktonic diatoms occurs at ca. 1.0 cal ka BP, where *A. granulata* and *Staurosira* spp. peak at up to 15 % and 25 % relative abundance, respectively, before *C. ocellata* dominates again at ca 0.6 cal ka BP. A distinct shift to increased abundance of the small *C. minuscula* occurs towards the top of the sequence at the expense of *C. paraocellata* and *C. prespanensis*. Most notably, a recent trend towards a marked increase in the benthic species *Cavinula scutelloides* (Smith) Lange-Bertalot occurs from 0.3 cal ka BP for the first time in the sequence, reaching a maximum of ca. 40% at ca. 0.05 cal ka BP, where benthic taxa dominate at > 60 %. In contrast, the surface sediment sample is dominated to >80% by *C. ocellata*, accompanied by the fragile, eutraphentic taxon *Nitzschia subacicularis* Hustedt.

Significant negative correlation in Spearman's Rank (Table 2), between the relative abundance of *C. paraocellata* and potassium (K) concentration (ρ = –0.7; confidence level = 91%) and positive correlation between *C. paraocellata* and total organic carbon (TOC) (ρ = 0.7; confidence level = 93%) was obtained. Results of DCA (Fig. 3, Table 3) indicate that Axis 1 scores track very closely the variation in % plankton, which is thus the most important element of variation in the diatom data.

5. Discussion

As an interpretive tool, the significant negative correlation between *C. paraocellata* and K concentration, a proxy for detrital input from the catchment (Aufgebauer et al. 2012), suggests that this species may dominate during clear water phases of low detrital input. We interpret *C. ocellata* and *C. paraocellata* here, as indicative of an oligotrophic-mesotrophic state, since *C. ocellata* is dominant in Lake Ohrid under similar low-nutrient conditions (Reed et al. 2010, Cvetkoska et al. 2012) and it has been suggested that the *Cyclotella* species are good competitors under stable and nutrient-diluted conditions (Winder et al. 2009). Overall, the DCA results suggest that lake-level change is the dominant influence on diatom species assemblage composition. The greater signature of hydrological change over productivity shifts is supported ecologically by the restricted dominance of more eutrophic taxa (e.g. *A. granulata*, *S. rotula*) to phases of greater relative abundance of benthic taxa, indicative of lower lake levels. Inferred deep water phases are dominated by taxa with low nutrient preferences, indicating that the increased relative abundance of plankton will not have been driven by a productivity-driven increase in absolute abundance of algae.

5.1. Late Glacial (17.1–15.7 cal ka BP)

PDZ 1 correlates closely with lithological unit LZ 1 (Aufgebauer et al. 2012), underlining the strong response to Late Glacial climate change (Figs 3, 4). The dominance of small Fragilariaceae, which often characterize shallow, unstable lake phases (Brugam et al. 1998, Jones & Birks 2004, Stone et al. 2011) is consistent with low productivity and a relatively short ice-free growing season, in a shallow lake phase of cold, dry climate. The abundance of benthic taxa also supports this, dominated by taxa with large, heavily-silicified valves, such as *C. marginatus*, *Surirella* spp. and *G. macedonicum*, which are found at depths of 15-17m within the organic epipelon of the modern lake (Levkov et al. 2007). This is completely in accord with the pollen record, dominated by sparse chenopod-*Artemisia* steppe vegetation (Panagiotopoulos et al. 2013).

5.2. Late Glacial to Holocene transition (15.7–11.5 cal ka BP)

The transition towards increased planktonic abundance at ca. 15.7 cal ka BP corroborates previous inferences of increased productivity based on total nitrogen (TN) and total organic carbon (TOC) (Aufgebauer et al. 2012), particularly in the peak of mesotrophic *S. rotula* at ca. 15.2 cal ka BP. *Stephanodiscus* species can generally tolerate low light conditions and Si availability, but require high phosphorus supply (Kilham et al. 1986). Most notably, the trend towards increasing dominance of planktonic *Cyclotella* taxa indicates a gradual increase in lake level for which - in the absence of sufficient carbon - hydrological proxy data were previously absent (Leng et al. 2013). Diatom inferences for lake response (lake level) match clearly with catchment-based palynological inferences of a gradual increase in temperature and precipitation from evidence for the expansion of trees (Panagiotopoulos et al. 2013).

Supporting previous inferences concerning definition of the Late Glacial interstadial-stadial boundary, zone PDZ 3 (13.1–12.3 cal ka BP) signals significant changes in the diatom flora during the Younger Dryas (’YD’), although being represented only by two samples. According to the age model, it has an earlier onset than in most sites, where the event tends to occur from 12.8 to 11.7 ka.

The dominance of *A. granulata* at the start of the zone is surprising, but the return to dominance of *S. pinnata* in the upper sample is clearly consistent with a glacial-type environment. *Aulacoseira granulata* is a clear indicator of eutrophic, turbid conditions with low light penetration (Kilham et al. 1986) and it is often found in shallow and wind stressed eutrophic waters (Stoermer & Ladewski, 1976). Its dominance has been also interpreted as indictive of shallow lake-level phases in several studies elsewhere (Gaillard et al. 1991, Dong et al. 2008, Stone et al. 2011). It is possible that the nutrient pulse is linked to enhanced catchment erosion due to a combination of lake-level reduction, wind stress and, possibly, to wider catchment erosion linked to the reversal to a chenopod-*Artemisia* steppe at this time reported by Panagiotopoulos et al. (2013). Thus, the diatom data support previous inferences and provide strong evidence for climatic reversal during the Younger Dryas event (cf. Alley 2000).

Unlike in many other records, where the Holocene transition is represented by a major, abrupt transition (Björk et al. 1998, Wilson et al. 2008), the diatom data support previous inferences in indicating an unusually gradual transition. According to the age model, a trend to warmer and wetter conditions starts at ca. 12.3 cal ka BP, prior to the classic transition date of 11.7 cal ka BP. This is represented in PDZ 4a by peak abundance of *S. rotula* and moderate renewed abundance of *Cyclotella* taxa, but with the maintenance of small Fragilariaceae. The high inferred nutrient supply in PDZ 4a indicated by *S. rotula* matches high K concentration and again corroborates previous inferences of enhanced catchment erosion, supported by the continued presence of ice-rafted debris (IRD). The associated (and slightly earlier) shift towards increased thermophilous vegetation (Panagiotopoulos et al. 2013) supports associated warming, but is at odds with the IRD signal. High plankton abundance (>80%) is achieved only in PDZ4b, after 11.0 cal ka BP.

5.3. The Early Holocene (11.5–7.9 cal ka BP)

The early Holocene period in the diatom record (subzones PDZ 4b and PDZ 4c; ca. 11.5–7.9 cal ka BP) correlates well with lithozones LZ 3a–LZ 3c (Aufgebauer et al. 2012). A trend towards decreasing productivity is suggested by the declining abundance of *S. rotula*, and is slightly at odds with previous inferences of high productivity based on increased TOC and TN content.

The marked transition to planktonic dominance (70–>80%) at the expense of small Fragilariales represents very strong proxy evidence for rapid lake-level increase. The lake responded more rapidly to increased moisture availability than the catchment vegetation, which shows a more gradual expansion of thermophilic and moisture-demanding taxa, such as *Tilia*, *Fraxinus*, *Ulmus* and *Fagus* and a delay in the loss of steppic *Artemisia* and Chenopodiaceae (Panagiotopoulos et al. 2013). Most importantly, the period ca. 10.0–8.0 ka is marked out in the stable isotope data as an arid phase of enhanced evaporative concentration, with high positive δ^{18}O values. In combination, the diatom and palynological data point instead to rapid wetting after the start of the Holocene. This has important implications for the debate concerning the spatial variability of moisture availability across the Mediterranean, standing in contrast to the palynologically-based argument that the northern Mediterranean was largely arid at the onset of the Holocene (Tzedakis, 2007).

Changes in the *C. ocellata* /*C. paraocellata* abundance ratio occur thereafter, in a sustained phase of high lake levels peaking at ca. 7.9–6.0 cal ka BP. The predominance of *C. paraocellata* indicates a low-nutrient, clear water state with low detrital input. In a similar manner to the previous phase, this is slightly at odds with the high nutrient status from 9.3 to 8.3 ka inferred previously (Aufgebauer et al. 2012), possibly relating in part to the effects of differential preservation of organic matter in other parts of the record. A minor increase in benthic taxa in a single sample at ca. 8.4 cal ka BP may represent lake-level reduction leading up to the 8.2 ka event, but could simply be a function of higher water transparency. More convincingly, a minor increase of the proportion of benthic taxa and a distinct peak of the small taxon, *C. minuscula*, at ca. 8.0 cal ka BP correlates with a peak in K counts indicative of enhanced fine clastic sediment supply, and also with a minor increase in *Artemisia* (Aufgebauer et al. 2012, Panagiotopoulos et al. 2013). These minor shifts have previously been interpreted tentatively as the impact of the abrupt Northern Hemisphere 8.2 ka climatic reversal (Bond et al. 1997, Mayewski et al. 2004, Lowe et al. 2008). There is no equivalent shift in oxygen stable isotope values (Leng et al. 2013), so the definition of this event remains rather tenuous.

5.4. Mid Holocene (7.9–1.9 ka calBP)

The mid Holocene (PDZ 4d; 7.9–1.9 cal ka BP) correlates well with the lithological unit LZ–3d. The peak in planktonic taxa of up to 95 % from ca. 7.9 to 6.0 cal ka BP represents maximum Holocene lake levels and is important in delineating the mid Holocene as the period of maximum moisture availability in Lake Prespa. Warmer temperatures and a relatively high trophic state can be inferred from the geochemical and pollen data. In the diatom record the continued presence of *S. rotula* at low abundance lends some support, but the sustained dominance of the *C. paraocellata* and the *C. ocellata* complex, and the absence of more eutrophic taxa such as *A. granulata,* is more indicative of the maintenance of trophic state within the oligo–mesotrophic range. This is also supported by the low sediment accumulation rate indicative of reduced productivity.

Importantly, the maintenance of high lake levels until 1.9 cal ka BP, and the peak of inferred humidity from ca. 7.9–6.0 cal ka BP, correlates closely with the oxygen stable isotope profile. This confirms that the latter is driven primarily by evaporative concentration rather than reflecting regional shifts in precipitation sources over time, between the Mediterranean Sea and central Europe, an alternate hypothesis presented by Leng et al. (2013). Within this, there is no evidence for a response to well-known episodes of rapid climate change across the Northern Hemisphere between 4.2–3.8 cal ka BP and 3.5–2.5 cal ka BP (Mayewski et al. 2004). In the light of the muted response to the 8.2 ka event, this is not surprising since it is a deep, well-buffered lake during this time.

The impact of human activities needs to be considered in the later Holocene. There is evidence for intensified human impact across the Balkans at the end of the Late Bronze Age, at ca. 2.8 ka BP in particular (Roberts et al. 2011a). The pollen record shows evidence for human-induced deforestation around Lake Prespa at ca. 2.0 cal ka BP (Panagiotpoulos et al. 2013). The results of archaeological excavations around Lake Ohrid (Kuzman 2010) indicate expanded human occupation at ca. 2.2 ka BP, and with palynological evidence for anthropogenic deforestation of the lake's catchment from 2.4 ka (Wagner et al. 2009, Vogel et al. 2010). Taking into account the proximity of the two lakes, it is reasonable to assume similar land-use characteristics in both catchments, with accelerated human impact from ca. 2.4 – 2.0 cal ka BP. In spite of this, our data indicate no major impact on either lake levels or productivity.

5.5. Late Holocene (1.9 cal ka BP–present)

The late Holocene (PDZ 5; 1.9 cal ka BP–present) is characterized by diatom-inferred lake-level fluctuation and increased trophic status. The decreased abundance of *C. paraocellata* and *C. prespanensis* for the first time since the early Holocene suggests that the lake has undergone strong human pressure during the late Holocene from anthropogenic activities leading to eutrophication. This is supported by the increased TOC, Fe/Ti and C/N and shifts in ostracod species assemblage composition (Aufgebauer et al. 2012). The pollen record shows increased abundance of herb and crop pollen and intensified agriculture at ca. 1.9 cal ka BP. A peak in the small planktonic taxon *C.*

minuscula correlates with a peak in K at ca. 1.5 cal ka BP, probably as a result of increased soil erosion due to forest clearance as interpreted from the sediment record.

Based on inferences derived from the pollen record, Panagiotopoulos et al. (2013) suggested changes in precipitation over the catchment were not distinct since increased abundance of moisture-demanding *Fagus* substitutes for the decline of the climax *Abies* forest. However, as in the earlier Holocene, the two clear phases of decreased plankton abundance in the diatoms, summarized well in the DCA Axis 1 Sites scores, correlate well with phases of increased *Artemisia* and chenopod abundance, implying a clear local decrease in the moisture availability. These phases peak at 1.0 cal ka BP and at ca. 0.05 cal ka BP (ca. 100 years ago). The arid episode at ca. 1.0 cal ka BP also exhibits peaks of eutrophic *A. granulata* and *Staurosira* spp. indicative of accelerated anthropogenic nutrient input. *Aulacoseira granulata* is common in Prespa's modern eutrophic diatom flora, and *Staurosira* spp. are mainly of benthic or epiphytic life habit, being abundant in the littoral zone of the modern lake (Levkov et al. 2007). Renewed plankton dominance suggests increased moisture availability between the two minima (ca. 1.0 – 0.05 cal ka BP), and matches with increased abundance of *Abies* in the pollen record (Panagiotoloulos et al. 2013). The second inferred lake-level drop at ca. 0.05 cal ka BP is marked by a shift to >40% of the benthic cosmopolitan species *C. scutelloides*. This species is often found in sandy, alkaline environments (Cumming et al. 1995, Jewson et al. 2006). In the recent flora of the lake, the benthic communities on sand substrate and silicate bedrock are dominated by *C. scutelloides* (Levkov et al. 2007). In the modern surface sample, a complete domination of *C. ocellata* and the appearance of the more eutrophic taxon *Nitzschia subacicularis* reflects increased P loading through the intensified human impact, mainly agricultural, as also pointed by Matzinger et al. (2006).

There is some evidence for increased temperatures followed by subsequent aridification and lake level decline between ca. 1.5–0.6 cal ka BP in the sediment and stable isotope record (Aufgebauer et al. 2012, Leng et al. 2013), while lake level almost 10 m lower than today has been inferred from the position of historical settlements originating from the end of the 10th and the beginning of the 11th century AD (Cvijic 1911, Sibinovic 1987). In conjunction, the proxy data now provide strong palaeoclimate data for phases of drought, possibly in the local catchment area rather than at higher altitude.

6. Comparison with regional and global records

The diatom proxy data of Prespa Co1215 are compared to selected proxies from Lake Ohrid, the Mediterranean region and Greenland ice-core data, in Fig.5.

6.1. Greenland Stadial 2 GS–2 (17.1–14.8 cal ka BP)

The diatom-inferred cold, arid Late Glacial (ca. 17.1–15.7 cal ka BP) in Prespa shows marked ecological similarity with the Late Glacial diatom records of other lakes in the region, including Lake Ohrid (Wagner et al. 2009, Reed et al. 2010), Lake Ioannina in semi-humid NW Greece (Wilson et al. 2008), and lake Les Echets, France (Ampel et al. 2008), in the dominance of small Fragilariales in alkaline water. In the western Mediterranean, sea surface temperature (SST) reconstructions for the Gulf of Cadiz, the Alboran and Tyrrhenian Sea indicate several climate oscillations during Heinrich event 1 (H1, ca. 19.0 –14.6 cal ka BP, e.g. Stanford et al. 2011). Temperatures 5–6 °C lower than in the Holocene and start of the deglaciation at ca. 16 cal ka BP, prior to the Greenland Interstadial (GI–1), are reconstructed for the Gulf of Cadiz (Cacho et al. 2001). The H1 event in the Aegean Sea was characterized by a cold and dry phase, which culminated at ca. 16.5 cal ka BP, and a milder phase starting at 15.7 cal ka BP (Kotthoff et al.

2011). Both events correlate closely with the minimum in plankton observed in PDZ 1 and the transition to PDZ 2a with warming/more humid conditions, respectively. In the Eastern Mediterranean region, global cooling and/or aridification at 16.5 cal ka BP was recorded in the $\delta^{18}O$ profile from Soreq Cave speleothems (Bar-Matthews et al. 1999). At the same time, inferred water-level drop with precipitation of a thick gypsum sequence occurred in Lake Lisan (Bartov et al. 2003).

6.2. Greenland Interstadial 1 GI–1 (14.8–12.7 cal ka BP) and GS–2 (12.7–11.5 cal ka BP)

Following initial warming and wet conditions from 15.7 cal ka BP, the maximum Late Glacial Prespa phase of water refill between 14.7–13.1 cal ka BP corresponds well to the more stable and humid climate conditions of the Bølling/Allerød (B/A) interstadial (cf. Mangerud et al. 1974, Björck et al. 1998). As noted, the strong diatom response is important in strengthening interpretation, in a phase where stable isotope data are of low reliability due to low TOC content in the sediment record (Leng et al. 2013). Since the Late Glacial of Ohrid sequences appear to be disturbed (Wagner et al. 2009; Reed et al. 2010) this is the first clear evidence for the Dessarets area, corresponding well with the summer precipitation curve for Lake Maliq (Bordon et al. 2009) and the early temperate phase inferred from pollen records of the Alboran and Aegean Sea between 14.7–13.0 ka BP (Dormoy et al. 2009). The Lake Prespa diatom record also compares well with the duration of more humid conditions in the East Mediterranean Region, ca. 15.0–12.0 cal ka BP, inferred from Soreq Cave speleothem data (Bar-Matthews et al. 1997).

The diatom-inferred climate reversal between 13.1–12.3 cal ka BP, and subsequent return to warming and increased humidity , confirms the impact on Lake Prespa of the Younger Dryas (YD) event. Further east, cool and drier conditions between 12.5–12.1 cal ka BP followed by increased moisture availability from 12.1–11.5 cal ka BP have been inferred for Lake Dojran, Macedonia (Francke et al. 2013). Across the Balkans, low water stands during the Younger Dryas were also indicated by the summer precipitation curve for Lake Maliq (Bordon et al. 2009) and from the dominance of *S. pinnata* prior to 12.5 ka in Lake Ioannina (Wilson et al. 2008). Pronounced aridity during the Younger Dryas was also indicated in the pollen record from the Alboran and Aegean Sea, with a temperature reduction of 3–5 °C during 12.4 to 12.2 cal ka BP suggested in the Aegean (Dormoy et al. 2009). There is various evidence for a more arid climate in the Eastern Mediterranean during the Younger Dryas strengthening understanding of an event which was previously poorly understood (Bottema, 1995). Overall, the Lake Prespa multi-proxy data correlate with events GI–1 and GS–2 of the Greenland ice-core isotope record (Björk et al. 1998).

6.3. Holocene period (11.5 cal ka BP – present)

As noted, the diatom-inferred trend towards a warming and more humid conditions from ca. 12.3 cal ka BP, before the classic Holocene transition at 11.5 ka (or 11.7 ka; cf. Rasmussen et al. 2006, Lowe et al. 2008), and its gradual character, is unusual. Between ca. 11.5–9.0 cal ka BP, after the start of the Holocene, the Lake Prespa diatom data correspond well to the Aegean Sea warm/cold% curve derived from planktonic foraminifera data (Rohling et al. 2002), the alkenone derived SST curve for the Adriatic Sea (Giunta et al. 2001) and the NGRIP oxygen isotope record (Andersen et al. 2006). This provides strong evidence for rapid increase in humidity, in contrast to the 10.0-8.0 cal ka BP arid event suggested by the oxygen stable isotope data.

The most prominent abrupt event during the early Holocene is at 8.2 ka. Here the diatoms match other indicators, and also other records from lakes Ohrid and Prespa (Lz1120 from Lake Ohrid and Co1204, a shallower-water core from Prespa; Holtvoeth et al. 2010; Wagner et al. 2009; 2010), in only providing subtle evidence for environmental impact. Stronger evidence for aridification and lake-level decline between ca. 8.3–7.9 cal ka BP was recorded for Macedonian Lake Dojran (Francke et al. 2013). However, it is possible that the signature is only strong in shallower, less well-buffered systems. In a similar vein, the pollen record from Tenaghi Philippon, a sensitive region of semi-arid climate, provides substantial evidence for climate-induced disturbance of terrestrial ecosystems correlated to the 8.2 ka event (Pross et al. 2009) than the semi-humid site of Lake Ioannina (Wilson et al. 2008). In central Italy, the pollen record from Lake Accesa demonstrates lake-level lowering between 8.6–7.9 (Drescher–Schneider et al. 2007). In the Western Mediterranean, a cooling trend with a decreased SST at ca. 8.2 ka was inferred from the sediment record of the Alboran Sea (Cacho et al. 2001). Rapid cooling and decreased precipitation at ca. 8.0 cal ka BP are also inferred from the Eastern Mediterranean region (Bar-Matthews et al.1997).

In Prespa, the maximum diatom-inferred humidity in the mid Holocene, with a trend to warming and wetting reaching a maximum between ca. 7.9–6.0 cal ka BP, followed by relatively high lake levels until ca. 1.9 ka, suggests that climate in this part of the Mediterranean is neither driving, nor being forced predominantly, by the Mediterranean Sea. The wetting trend correlates approximately with the timing of the S_1 sapropel formation in the Eastern Mediterranean (ca. 9.0–6.8 cal ka BP, cf. Ariztegui et al. 2000), also recognized as the wettest Holocene phase across the Levant and the Eastern Mediterranean (Robinson et al. 2006 and references therein), but endures for a longer duration. Transgression of the Adriatic Sea and sea level rise was suggested to have occurred at the time of the S_1 formation, followed by a subsequent aridification and increased salinity after ca. 6.0 cal ka BP (Siani et al. 2013). Decreased humidity after 6.0 ka BP has also been inferred elsewhere (Reed et al. 2001, Roberts et al. 2001, Barker et al. 2007, Desprat et al. 2013, Fletcher & Zielhofer 2013), possibly linked to the IRD event at 5.9 ka BP in the North Atlantic (Bond et al. 1997) and the "cool poles, dry tropics" Rapid Climate Change (RCC) event between 6.0–5.0 ka BP (Mayewski et al. 2004). Unlike many other circum-Mediterranean sites and in spite of inferences for a warm and dry climate between 6.4–2.4 cal ka BP derived from the highest calcite content in core Co1202 from neighboring Lake Ohrid (Vogel et al. 2010), the maintenance of relatively high lake levels after the maximum in Lake Prespa indicates closer correspondence with the pattern induced by North Atlantic forcing.

In the later Holocene, the anomalous abrupt event from 4.2–3.8 ka BP has received much attention, being defined as a classic cold/dry event linked to glacial retreat in Europe (Mayewski et al. 2004). The 4.2 ka event has no clear expression in Prespa, in spite of inferences of a colder and/or drier climate in lakes Ohrid (Wagner et al. 2009, Wagner et al. 2010, Vogel et al. 2010) and Dojran (Francke et al. 2013). In light of the above discussion, this is not surprising, since the diatoms may have reduced sensitivity in Prespa due to higher lake levels causing a buffering effect, similar as in Lake Eski Acigöl, Turkey, (Roberts et al. 2001),

The late Holocene in Lake Prespa is a period of intensified human impact superimposed on climate change, and the diatom data are important in disentangling climate change from human impact. The most prominent inferred climatic shift occurred at ca. 1.0 cal ka BP, when Lake Ohrid also shows evidence for aridification (Wagner et al. 2009, Vogel et al. 2010). Francke et al. (2013) reported an opposite situation for Lake Dojran, with higher water level, but caused primarily by anthropogenic impact. The change in Lake Prespa's hydrology could be connected with the 'Medieval Climatic Anomaly' which started at ca. AD 950- (ca. 1 ka, as here) (Mann 2002) as also reported from other records in the region (Allen et al. 2002, Chen et al. 2013, Nieto-Moreno 2013), being bolstered by a correlation with increased steppe vegetation suggesting aridification rather than human impact. It also correlates with a phase of reduced summer precipitation identified in Lake Maliq, Albania

(Bordon et al. 2009), which may now be defined as of regional significance. Arid conditions and forest decline in the western Mediterranean have been defined at ca.1.9 cal ka BP (Fletcher et al. 2013), in contrast to the northeastern region. Palaeolimnological data from the eastern Mediterranean reflect stronger deforestation during the Bronze Age, with a spatially variable signature occurring between ca. 5.0–3.3 cal ka BP in different localities such as Central Anatolia, Greece, Levant and Turkey (Roberts et al. 2011b).

The above comparison highlights an intriguing pattern in Lake Prespa's response to Holocene climate change. A close match to North Atlantic and records across the Mediterranean exists in the earlier warm and humid phase of the Holocene, at the time of increased summer monsoon and sapropel S_1 formation. In the mid-late Holocene (ca. 6.0 cal ka BP–present), Lake Prespa displays closer correlation to the wet phases observed in the lakes of central–west Italy (Magny et al. 2009, 2012, 2013, Vannière et al. 2013). This suggests a much closer link to NW European records and, somehow, to the influence of Atlantic forcing. As suggested by Fletcher et al. (2010) in presenting contrasting Late Quaternary data from the western and central Mediterranean, this study highlights again the complexity of the Mediterranean climate. Fletcher et al. (2010) suggest the differences may be explained by shifts in the intensity and position of the westerlies over western and central Europe, which are possibly associated with changing frequency of atmospheric highs over the European mid-latitudes.

7. Conclusions

The ca. 17 ka diatom sequence from Lake Prespa generates a strong proxy for lake-level change and strengthens considerably the power of the multi-proxy data-set for palaeoclimate reconstruction during the Late Glacial to Holocene. With clear evidence for a Younger Dryas climatic reversal, the most notable element of the Late Glacial record is the slow run up towards the Holocene transition, with a gradual increase in temperature and precipitation before more rapid lake-level increase during the early Holocene. Here, convincing evidence is provided that the Early Holocene was warm and wet, in contrast to inferences of aridity based on stable isotope data, and in contrast to the theory that the northern Mediterranean was arid at this time. The high lake levels thereafter until 1.9 ka and, by inference, moisture availability, show little affinity with the Eastern Mediterranean, where marked lake-level reduction occurs after the mid-Holocene. Instead, the lake-level curve matches the Greenland curve very closely, suggesting a teleconnection – somehow – with North Atlantic forcing. After 1.9 ka, two clear aridity events at ca. 1.0 ka and 100 years ago provide evidence for short-term climatic variability, against a backdrop of increasing nutrient status with accelerated anthropogenic impact.

Acknowledgements

The authors would like to thank the Alexander von Humboldt foundation for financial support of the project: “Reconstruction of past environmental variations in ancient Lake Ohrid, a diatom inferred perspective”; Paul B. Hamilton, Canadian Museum of Nature, for helpful discussions about palaeolimnology; Mrs Danijela Mitić Kopanja, Institute of Biology, Faculty of Natural Sciences, Skopje, Macedonia for technical assistance, Vasko Avukatov, Macedonian Ecological Society for providing the map.

8. References

Albrecht, C., Wilke, T., 2008. Ancient Lake Ohrid: biodiversity and evolution. Hydrobiologia 615, 103–140.

Allen, J.R.M., Brandt, U., Brauer, A., Hubberten, H.W., Huntley, B., 1999. Rapid environmental changes in southern Europe during the last glacial period, Nature 400, 740–743. Allen, J.R.M., Watts, W.A., McGee, E., Huntley, B., 2002. Holocene environmental variability – the record from Lago Grande di Monticchio, Italy. Quaternary International 88, 69–80.

Alley, R.B., 2000. The Younger Dryas cold interval as viewed from central Greenland. Quaternary Science Reviews 19, 213–226.

Ampel, L., Wohlfarth, B., Risberg, J., Veres, D., 2008. Paleolimnological response to millennial and centennial scale climate variability during MIS 3 and 2 as suggested by the diatom record in Les Echets, France. Quaternary Science Reviews 27, 1493–1504.

Andersen, K.K., Svensson, A., Rasmussen, S.O., Steffensen, J.P., Johnsen, S.J., Bigler, M., Röthlisberger, R., Ruth, U., Siggaard-Andersen, M.L., Dahl-Jensen, D., Vinther, B.M., Clausen, H.B., 2006. The Greenland Ice Core Chronology 2005, 15–42 ka. Part 1: constructing the time scale. Quaternary Science Reviews 25, 3246–3257.

Ariztegui, D., Asioli, A., Lowe, J.J., Trincardi, F., Vigliotti, L., Tamburini, F., Chondrogianni, C., Accorsi, C.A., Bandini Mazzanti, M., Mercuri, A.M., Van der Kaars, S., McKenzie, J.A., Oldfield, F., 2000. Palaeoclimate and the formation of sapropel S1: inferences from Late Quaternary lacustrine and marine sequences in the central Mediterranean region. Palaeogeography, Palaeoclimatology, Palaeoecology 158, 215–240.

Aufgebauer, A., Panagiatopoulos, K., Wagner, B., Schäbitz, F., Viehberg, F.A., Vogel, H., Zanchetta, G., Sulpizio, R., Leng, M.J., Damaschke, M., 2012. Climate and environmental change in the Balkans over the last 17 ka recorded in sediments from Lake Prespa (Albania/F.Y.R. of Macedonia/Greece). Quaternary International 274, 122–135.

Barker, P., Leng, M.J., Gasse, F., Huang, Y., 2007. Century-to-millennial scale climatic variability in Lake Malawi revealed by isotope records. Earth and Planetary Science Letters 261, 93–103.

Bar-Matthews M., Ayalon A., Kaufman A.,1997. Late Quaternary paleoclimate in the eastern Mediterranean region from stable isotope analysis of speleothems at Soreq Cave, Israel. Quaternary Research 47, 155–168.

Bar-Matthews, M., Ayalon, A., Kaufman, A., Wasserburg, G.J., 1999. The Eastern Mediterranean palaeoclimate as a reflection of regional events: Soreq cave, Israel. Earth and Planetary Science Letters 166, 85–95.

Bar-Matthews, M., Ayalon, A., Gilmour, M., Matthews, A., Hawkesworth, C.J., 2003. Sea-land oxygen isotopic relationships from planktonic foraminifera and speleothems in the Eastern Mediterranean region and their implication for paleorainfall during interglacial intervals, Geochimica et Cosmochimica Acta 67, 3181–3199.Bartov, Y., Goldstein, S.L., Stein, M., Enzel, Y., 2003. Catastrophic arid episodes in the Eastern Mediterranean linked with the North Atlantic Heinrich events. Geology 31, 439-442.

Battarbee, R.W., 1986. Diatom analysis. In Berglund, B. E. (ed.), Handbook of Holocene Palaeoecology and Palaeohydrology. J. Wiley & Sons, Chichester, 527–570.

Björck, S., Walker, M.J.C., Cwynar, L., Johnsen, S.J., Knudsen, K-L., Lowe, J.J., Wohlfarth, B., INTIMATE Members, 1998. An event stratigraphy for the Last Termination in the North Atlantic region based on the Greenland Ice Core record: a proposal by the INTIMATE group. Journal of Quaternary Science 13, 283–292.

Bond, G., Showers, W., Cheseby, M., Lotti, R., Almasi, P., DeMenocal, P., Priore, P., Cullen, H., Hajdas, I., Bonani, G., 1997. A pervasive millenial-scale cycle in North Atlantic Holocene and glacial climates. Science 278, 1257–1266.

Bordon, A., Peyron, O., Lézine, A.M., Brewer, S., Fouache, E., 2009. Pollen-inferred Late-Glacial and Holocene climate in southern Balkans (Lake Maliq). Quaternary International 200, 19–30.

Bottema, S., 1995. The Younger Dryas in the eastern Mediterranean. Quaternary Science Reviews 14, 883–891.

Bourcart, J., 1922. Les confins albanais administre´s par la France. Revue de Geographie 10, 307pp.

Brugam, R.B., McKeever, K., Kolesa, L., 1998. A diatom-inferred water depth reconstruction for an Upper Peninsula Michigan, lake. Journal of Paleolimnology 20, 267–276.

Cacho, I., Grimalt, J.O., Canals, M., Sbaffi, L., Shackleton, N.J., Schönfeld, J., Zahn, R., 2001. Variability of the western Mediterranean Sea surface temperature during the last 25,000 years and its connection with the Northern Hemisphere climatic changes. Paleoceanography 16, 40–52.

Cacho, I., Grimalt, J. O., Canals, M., 2002. Response of the Western Mediterranean Sea to rapid climate variability during the last 50,000 years: a molecular biomarker approach. Journal of Marine Systems 33, 253–272.

Chen, L., Zonneveld, K.A.F., Versteegh, G.J.M., 2013. Paleoclimate of the Southern Adriatic Sea region during the 'Medieval Climate Anomaly' reflected by organic walled dinoflagellate cysts. The Holocene 0(0) 1–11. in press.

Cumming, B.F., Wilson, S.E., Hall, R.I., Smol, J.P., 1995. Diatoms from British Columbia (Canada) lakes and their relationship to salinity, nutrients and other limnological variables. Bibliotheca Diatomologica 31, 1–207.

Cvetkoska, A., Hamilton, P. B., Ognjanova-Rumenova, N., Levkov, Z. Observations of the genus *Cyclotella* (Kützing) Brébisson in ancient lakes Ohrid and Prespa and a description of two new species *C. paraocellata* spec. nov. and *C. prespanensis* spec. nov. Nova Hedwigia, in press. doi: 10.1127/0029-5035/2014/0154.

Cvetkoska, A., Reed, J.M., Levkov, Z., 2012. Diatoms as indicators of environmental change in ancient Lake Ohrid during the last glacial-interglacial cycle (ca. 140 ka). In: Witkowski, A. (Ed.), Diatom Monographs Vol. 15. ARG Gartner Verlag, 220pp.

Cvijic, J., 1911. Fundamentals of geography and geology of Macedonia and Old Serbia. Book III, Serbian Academy of Sciences, Special Edition. – Beograd (in Serbian).

Damaschke, M., Sulpizio, R., Zanchetta, G., Wagner, B., Böhm, A., Nowaczyk, N., Rethemeyer, J., Hilgers, A., 2013. Tephrostratigraphic studies on a sediment core from Lake Prespa in the Balkans. Climate of the Past 9, 267–287.

Desprat, S., Combourieu-Nebout, N., Essallami, L., Sicre, M.A., Dormoy, I., Peyron, O., Siani, G., Bout Roumazeilles, V., Turon, J.L., 2013. Deglacial and Holocene vegetation and climatic changes in the southern Central Mediterranean from a direct land-sea correlation. Climate of the Past 9, 767–787.

Dong, X.H., Bennion, H., Battarbee, R., Yang, X.D., Yang, H.D., Liu, E.F., 2008. Tracking eutrophication in Taihu Lake using the diatom record: potential and problems. Journal of Paleolimnology 40, 413–429.

Dormoy, I., Peyron, O., Combourieu-Nebout, N., Goring, S., Kotthoff, U., Magny, M., Pross, J., 2009. Terrestrial climate variability and seasonality changes in the Mediterranean region between 15000 and 4000 years deduced from marine pollen records. Climate of the Past 5, 615–632.

Drescher-Schneider, R., De Beaulieu, J.L., Magny, M., Walter-Simonnet, A.V., Bossuet, G., Millet, L., Brugiapaglia, E., Drescher, A., 2007. Vegetation history, climate and human impact over the last 15,000 years at Lago dell' Accesa (Tuscany, Central Italy). Vegetation History and Archaeobotany 16 (4), 279–299.

Fletcher, W.J., Debret, M., Sanchez Goñi, M.F., 2013. Mid-Holocene emergence of a low frequency millennial oscillation in western Mediterranean climate: Implications for past dynamics of the North Atlantic atmospheric westerlies. The Holocene 23(2), 153–166.

Fletcher, W.J., Sanchez Goñi, M.F., Peyron, O., Dormoy, I., 2010. Abrupt climate changes of the last deglaciation detected in a Western Mediterranean forest record. Climate of the Past 6, 245–264.

Fletcher, W.J., Zielhofer, C., 2013. Fragility of Western Mediterranean landscapes during Holocene Rapid Climate Changes. Catena 103,16–29.

Francke, A., Wagner, B. Leng, M.J., Rethemeyer, J., 2013. A Late Glacial to Holocene record of environmental change from Lake Dojran (Macedonia, Greece). Climate of the Past 9, 481–498.

Gaillard, M.J., Dearing, J.A., E1-Daoushy, F., Enell, M., Håkansson, H., 1991. A late Holocene record of land-use history, soil erosion, lake trophy and lake-level fluctuations at Bjäresjösjön (South Sweden). Journal of Paleolimnology 6, 51-81.

Giunta, S., Emeis, K.C., Negri, A., 2001. Sea surface temperature reconstruction of the last 16000 years in the eastern Mediterranean Sea. Rivista Italiana di Paleontologia e Stratigrafia 107 (3), 463– 476.

González-Sampériz, P., Valero-Garcés, B.L., Moreno, A., Jalut, G., García-Ruiz, J.M., C. Martí-Bono, C., Delgado-Huertas, A., Navas, A., Otto, T., Dedoubat, J.J. 2006. Climate variability in the Spanish Pyrenees during the last 30,000 yr revealed by the El Portalet sequence. Quaternary Research 66, 38–52

Grimm, E.C., 1987. CONISS: a FORTRAN 77 program for stratigraphically constrained cluster analysis by the method of incremental sum of squares. Computers & Geosciences 13, 13–35.

Grimm, E.C., 1991. TILIA and TILIA-GRAPH. Illinois State Museum, Springfield, USA.

Håkansson, H., 1990. A comparison of *Cyclotella krammeri* sp. nov. and *C. schumannii* Håkansson stat. nov. with similar species. Diatom Research 5, 261–271.

Håkansson, H., 2002. A compilation and evaluation of species in the genera *Stephanodiscus*, *Cyclostephanos* and *Cyclotella* with a new genus in the family Stephanodiscaceae. Diatom Research 17, 1–139.

Hollis, G.E., Stevenson, A.C., 1997. The physical basis of the Lake Mikri Prespa systems: geology, climate, hydrology and water quality. Hydrobiologia 351, 1–19.

Holtvoeth, J., Vogel, H., Wagner, B., Wolff, G.A., 2010. Lipid biomarkers in Holocene and glacial sediments from ancient Lake Ohrid (Macedonia, Albania). Biogeosciences 7, 4607–4640.

Houk, V., Klee, R., Tanaka, H., 2010. Atlas of freshwater centric diatoms with a brief key and descriptions. Part 3. *Stephanodiscaceae* A. *Cyclotella*, *Tertiarius*, *Discostella*. Fottea 10 (Supplement),498pp.

Jewson, D.H., Lowry, S.F., Bowen, R., 2006. Co-existence and survival of diatoms on sand grains, European Journal of Phycology 41(2), 131–146.

Jones, V.J., Birks, H.J.B., 2004. Lake-sediment records of recent environmental change on Svalbard: results of diatom analysis. Journal of Paleolimnology 31, 445–466.

Jongman, R.H.G., ter Braak, C.J.F., van Tongeren, O.F.R., 1995. Data analysis in community and landscape ecology, Cambridge University Press, Cambridge, 324pp.

Juggins, S., 1991-2007. C2. User guide Version 1.5. Software for ecological and palaeoecological data analysis and visualization. School of Geography, Politics & Sociology. Newcastle University. Newcastle upon Tyne, UK. 73 pp.

Kilham, P., Kilham, S.S., Hecky, R.E., 1986. Hypothesized resource relationships among African planktonic diatoms. Limnology and Oceanography 31, 1169–1181.

Kiss, K.T., Klee, R., Hegevald, E., 1999. Reinvestigation of the original material of *Cyclotella ocellata* Pantocsek (Bacillariophyceae). Algological Studies 82, 39–53.

Kiss, K.T., Rojo, K., Cobelas, A.M., 1996. Morphological variability of a *Cyclotella ocellata* (Bacillariophyceae) population in the Lake Las Madres (Spain). Algological Studies 82, 37–55.

Kotthoff, U., Koutsodendris, A., Pross, J., Schmiedl, G., Bornemann, A., Kaul, C., Marino, G., Peyron, O., Schiebel, R., 2011. Impact of Lateglacial cold events on the northern Aegean region reconstructed from marine and terrestrial proxy data. Journal of Quaternary Science 26, 86–96.

Krammer, K., Lange-Bertalot, H. (2000). Centrales, Fragilariaceae, Eunotiaceae, In: Ettl, H., Gerloff, J., Heynig, H., Mollenhauer, D. (Eds.), Süßwasserflora von Mitteleuropa, 2/3, Gustav Fischer Verlag, Stuttgart, 599 pp (2nd edn).

Krammer, K., Lange-Bertalot, H., 1986. Bacillariophyceae 1. Teil: Naviculaceae. In: Ettl, H., Gerloff, J., Heynig, H., Mollenhauer, D. (Eds.), Süßwasserflora von Mitteleuropa, 2/1, Gustav Fischer Verlag, Stuttgart, 876 pp.

Krammer, K., Lange-Bertalot, H., 1991a. Bacillariophyceae 3. Teil: Centrales, Fragilariaceae, Eunotiaceae. In: Ettl, H., Gerloff, J. Heynig, H., Mollenhauer, D. (Eds), Süßwasserflora von Mitteleuropa, 2/3, Gustav Fischer Verlag, Stuttgart , 576 pp.

Krammer, K., Lange-Bertalot, H., 1991b. Bacillariophyceae 4. Teil: Achnanthaceae. Kritische Ergänzungen zu Navicula (Lineolatae) und Gomphonema. In: Ettl, H., Gärtner, G., Gerloff, J., Heynig, H., Mollenhauer, D., (Eds.), Süßwasserflora von Mitteleuropa, 2/4, Gustav Fischer Verlag, Stuttgart, 437 pp.

Krammer, K., Lange-Bertalot, H.,1997. Bacillariophyceae 2. Teil: Bacillariaceae, Epithemiaceae, Surirellaceae. In: Ettl, H., Gerloff, J., Heynig, H., Mollenhauer, D. (Eds.), Süßwasserflora von Mitteleuropa, 2/2, Gustav Fischer Verlag, Stuttgart, 536 pp.

Kuzman, P., May/June (2010). Plaoshnik–Ohrid. Macedonian Archaeological News Number 7, II, 2010. Electronic newsletter, joint project of the Cultural Heritage Protection Office of the Republic of Macedonia and the Institute for Social Sciences and Humanities Euro-Balkan. http://www.mav.mk/article.php?lang=en&article=42 (accessed 20.07.13).

Leng, M.J., Baneschi, I., Zanchetta, G., Jex, C.N., Wagner, B., Vogel, H., 2010. Late Quaternary palaeoenvironmental reconstruction from Lakes Ohrid and Prespa (Macedonia/Albania border) using stable isotopes. Biogeosciences 7, 3109–3122.

Leng, M.J., Wagner, B., Boehm, A., Panagiotopoulos, K., Vane, C.H., Snelling, A., Haidon, C., Woodley, E., Vogel, H., Zanchetta, G., Baneschi, I., 2013. Understanding past climatic and hydrological variability in the Mediterranean from Lake Prespa sediment isotope and geochemical record over the Last Glacial cycle, Quaternary Science Reviews 66, 123-136.

Levkov, Z., Krstic, S., Metzeltin, D., Nakov, T., 2007. Diatoms of Lakes Prespa and Ohrid. About 500 taxa from ancient lake system. Iconographia Diatomologica 16, ARG Gartner Verlag, 603pp.

Lowe, J.J., Rasmussen, S.O., Björck, S., Hoek, W.Z., Steffensen, J.P., Walker, M.J.C., Yu, Z.C., The INTIMATE group, 2008. Synchronisation of palaeoenvironmental events in the North

Atlantic region during the Last Termination: a revised protocol recommended by the INTIMATE group. Quaternary Science Reviews 27 (1–2), 6–17.

Magny, M., Combourieu Nebout, N., de Beaulieu, J. L., Bout-Roumazeilles, V., Colombaroli, D., Desprat, S., Francke, A., Joannin, S., Peyron, O., Revel, M., Sadori, L., Siani, G., Sicre, M. A., Samartin, S., Simonneau, A., Tinner, W., Vanni`ere, B., Wagner, B., Zanchetta, G., Anselmetti, F., Brugiapaglia, E., Chapron, E., Debret, M., Desmet, M., Didier, J., Essallami, L., Galop, D., Gilli, A., Haas, J. N., Kallel, N., Millet, L., Stock, A., Turon, J. L., Wirth, S. 2013. North–south palaeohydrological contrasts in the central Mediterranean during the Holocene: tentative synthesis and working hypotheses, Climate of the Past Discuss. 9, 1901–1967, doi:10.5194/cpd-9-1901-2013.

Magny, M., Joannin, S., Galop, D., Vanniere, B., Haas, J. N., Basseti, M., Bellintani, P., Scandolari, R., and Desmet, M., 2012. Holocene palaeohydrological changes in the Northern Mediterranean borderlands as reflected by the lake-level record of Lake Ledro, Northeastern Italy. Quaternary Research 77, 382–396.

Magny, M., Vannière, B., Zanchetta, G., Fouache, E., Touchais, G., Petrika, L., Coussot, C., Walter-Simonnet, A.V., Arnaud, F., 2009. Possible complexity of the climatic event around 4300–3800 cal. BP in the central and western Mediterranean. The Holocene 19, 1–11.

Mangerud, J., Andersen, S.T., Berglund, B.E., Donner, J.J., 1974. Quaternary stratigraphy of Norden, a proposal for terminology and classification. Boreas 3, 109–128.

Mann, M.E., 2002. Medieval Climatic Optimum.The Earth system: physical and chemical dimensions of global environmental change. MacCracken, M.C., Perry, J.S., (Eds.) In:

Encyclopedia of Global Environmental Change. John Wiley & Sons, Ltd, Chichester. Vol.1. 514–516.

Matzinger, A., Spirkovski, Z., Patceva, S., Wüest, A., 2006. Sensitivity of ancient Lake Ohrid to local anthropogenic impacts and global warming. Journal of Great Lakes Research 32, 158–179.

Mayewski, P.A., Rohling, E.E., Stager, J.C., Karlen, W., Maasch, K.A., Meeker, L.D., Meyerson, E.A., Gasse, F., van Kreveld, S., Holmgren, K., 2004. Holocene climate variability, Quaternary Research 62, 243–255.

Nieto-Moreno, V., Martinez-Ruiz, F., Giralt, S., Gallego-Torres, D., García-Orellana, J., Masqué, P., Ortega-Huertas., 2013. Climate imprints during the 'Medieval Climate Anomaly' and the 'Little Ice Age' in marine records from the Alboran Sea basin. The Holocene doi: 10.1177/0959683613484613. in press.

Panagiotopoulos, K., Aufgebauer, A., Schäbitz, F., Wagner, B., 2013. Vegetation and climate history of the Lake Prespa region since the Lateglacial. Quaternary International 15 doi:10.1016/j.quaint.2012.05.048, in press.

Pross, J., Kotthoff, U., Müller, U.C., Peyron, O., Dormoy, I., Schmiedl, G., Kalaitzidis, S., Smith, A.M., 2009. Massive perturbation in terrestrial ecosystems of the Eastern Mediterranean region associated with the 8.2 kyr B.P. climatic event. Geology 10, 887–890.

R Core Team, 2012. R: A language and environment for statistical computing. R Foundation for Statistical Computing, Vienna, Austria. ISBN 3-900051-07-0, URL http://www.R project.org/.

Radoman, P., 1985. Hydrobioidea a superfamily Prosobranchia (Gastropoda), II. Origin, Zoogeography, Evolution in the Balkans and Asia Minor. Monographs Institute of Zoology 1, Beograd.

Rasmussen, S.O., Andersen, K.K., Svensson, A.M., Steffensen, J.P., Vinther, B.M., Clausen, H. B., Siggaard-Andersen, M.L., Johnsen, S.J., Larsen, L.B., Dahl-Jensen, D., Bigler, M., Röthlisberger, R., Fischer, H., Goto-Azuma, K., Hansson, M.E., RUTH, U., 2006. A new Greenland ice core chronology for the last glacial termination, Journal of Geophysical Research, 111, D06102, doi:06110.01029/02005JD006079.

Reed, J.M., Cvetkoska, A., Levkov, Z., Vogel, H., Wagner, B., 2010. The last glacial-interglacial cycle in Lake Ohrid (Macedonia/Albania): testing diatom response to climate. Biogeosciences 7, 3083–3094.

Reed, J.M., Stevenson, A.C., Juggins, S., 2001. A multi-proxy record of Holocene climatic change in southwestern Spain: the Laguna de Medina, Cádiz. The Holocene 11, 6, 707–719.

Renberg, I., 1990. A procedure for preparing large sets of diatom slides from sediment cores. Journal of Paleolimnology 4, 87–90.

Roberts, N., Brayshaw, D., Kuzucuoglu, C., Perez, R., Sadori, L., 2011a. The mid-Holocene climatic transition in the Mediterranean: Causes and consequences. The Holocene 21(1) 3–13.

Roberts, N., Eastwood, W.J., Kuzucuoglu, C., Fiorentino, G., Caracuta, V., 2011b. Climatic, vegetation and cultural change in the eastern Mediterranean during the mid-Holocene environmental transition. The Holocene 21(1), 147–162.

Roberts, N., Reed, J.M., Leng, M.J., Kuzucuoglu, C., Fontugne, M., Bertaux, J., Woldring, H., Bottema, S., Black, S., HUNT, E., Karabiyikoglu, M., 2001. The tempo of Holocene climatic change in the eastern Mediterranean region: new high-resolution crater-lake sediment data from central Turkey. The Holocene 11(6), 721–736.

Robinson, S.A., Black, S., Sellwood, B.W., Valdes, P.J., 2006. A review of palaeoclimates and palaeoenvironments in the Levant and Eastern Mediterranean from 25,000 to 5000 years BP: setting the environmental background for the evolution of human civilization. Quaternary Science Reviews 25, 1517–1541.

Rohling, E.J., Mayewski, P.A., Hayes, A., Abu-Zied, R.H., Casford, J.S.L., 2002. Holocene atmosphere–ocean interactions: records from Greenland and the Aegean Sea. Climate Dynamics 18, 587–593.

Siani, G., Magny, M., Paterne, M., Debret, M., Fontugne, M., 2013. Paleohydrology reconstruction and Holocene climate variability in the South Adriatic Sea. Climate of the Past 9, 499–515.

Shah, A., Morrill, C., Gille, E.P., Gross, W.S., Anderson, D.M., Bauer, B.A., Buckner, R., Hartman. M., 2011. Global speleothem oxygen isotope measurements since the Last Glacial Maximum. National Oceanic and Atmospheric Administration's National Climatic Data Center, Boulder, Colorado, USA. Accessed on 12/14/2011 from ftp://ftp.ncdc.noaa.gov/pub/data/paleo/syntrace/speleothem/speleothem-d18o-0-22k.csv.

Sibinoviç, M., 1987. Ezera Prespansko i Ohridsko. The SRC & Agency of Water Resources of R. of Macedonia, Skopje (in Macedonian).

Stanford, J.D., Rohling, E.J., Bacon, S., Roberts, A.P., Grousset, F.E., Bolshaw, M., 2011. A new concept for the paleoceanographic evolution of Heinrich event 1 in the North Atlantic. Quaternary Science Reviews 30, 1047–1066.

Stankovic, S., 1960. The Balkan Lake Ohrid and its living world. Monogr. Biol. IX. Uitgeverij Dr. W. Junk, Den Haag, Netherlands.

Stoermer, E.F., Ladewski, T.B., 1976. Apparent optimal temperatures for the occurrence of some common phytoplankton species in southern Lake Michigan. University of Michigan, Great Lakes Research Division Publications 18. 48 pp.

Stone, J.R., Westover, K.S., Cohen, A.S., 2011. Late Pleistocene paleohydrography and diatom paleoecology of the central basin of Lake Malawi, Africa. Palaeogeography, Palaeoclimatology, Palaeoecology 303, 51–70.

Tzedakis, P.C., 2007. Seven ambiguities in the Mediterranean palaeoenvironmental narrative. Quaternay Science Reviews 26, 2042–2066.

Vannière, B., Magny, M., Joannin, S., Simonneau, A., Wirth, S. B., Hamann, Y., Chapron, E., Gilli, A., Desmet, M., Anselmetti, F. S., 2013. Orbital changes, variation in solar activity and increased anthropogenic activities: controls on the Holocene flood frequency in the Lake Ledro area, Northern Italy, Clim. Past 9, 1193–1209, doi:10.5194/cp-9-1193-2013.Vogel, H., Wagner, B., Zanchetta, G., Sulpizio, R., Rosén, P., 2010. A palaeoclimate record with tephrochronological age control for the last glacial-interglacial cycle from Lake Ohrid, Albania and Macedonia. Journal of Paleolimnology 44, 295–310.

Wagner, B., Aufgebauer, A., Vogel, H., Zanchetta, G., Sulpizio, R., Damaschke, M., 2012. Late Pleistocene and Holocene contourite drift in Lake Prespa Albania/ F.Y.R. of Macedonia/Greece. Quaternary International 274, 112–121.

Wagner, B., Lotter, A.F., Nowaczyk, N., Reed, J.M., Schwalb, A., Sulpizio, R., Valsecchi, V., Wessels, M., Zanchetta, G., 2009. A 40.000-year record of environmental change from ancient Lake Ohrid (Albania and Macedonia). Journal of Paleolimnology 41, 407–430.

Wagner, B., Reicherter, K., Daut, G., Wessels, M., Matzinger, A., Schwalb, A., Spirkovski, Z., Sanxhaku, M., 2008. The potential of Lake Ohrid for long-term palaeoenvironmental reconstructions. Palaeogeography, Palaeoclimatology, Palaeoecology 259, 341–356.

Wagner, B., Vogel, H., Zanchetta, G., Sulpizio, R., 2010. Environmental changes on the Balkans recorded in the sediments from lakes Prespa and Ohrid. Biogeosciences 7, 3365–3392.

Wilson, G.P., Reed, J.M., Lawson, I.T., Frogley, M.R., Preece, R.C., Tzedakis, P.C., 2008. Diatom response to the last glacialinterglacial transition in the Ioannina basin, northwest Greece: implications for Mediterranean palaeoclimate reconstruction. Quaternary Science Reviews 27, 428–440.

Winder, M., Reuter, J.E., Schladow, S.G., 2009. Lake warming favours small-sized planktonic diatom species. Proceedings of the Royal Society of Biological Sciences, 276, 427–435.

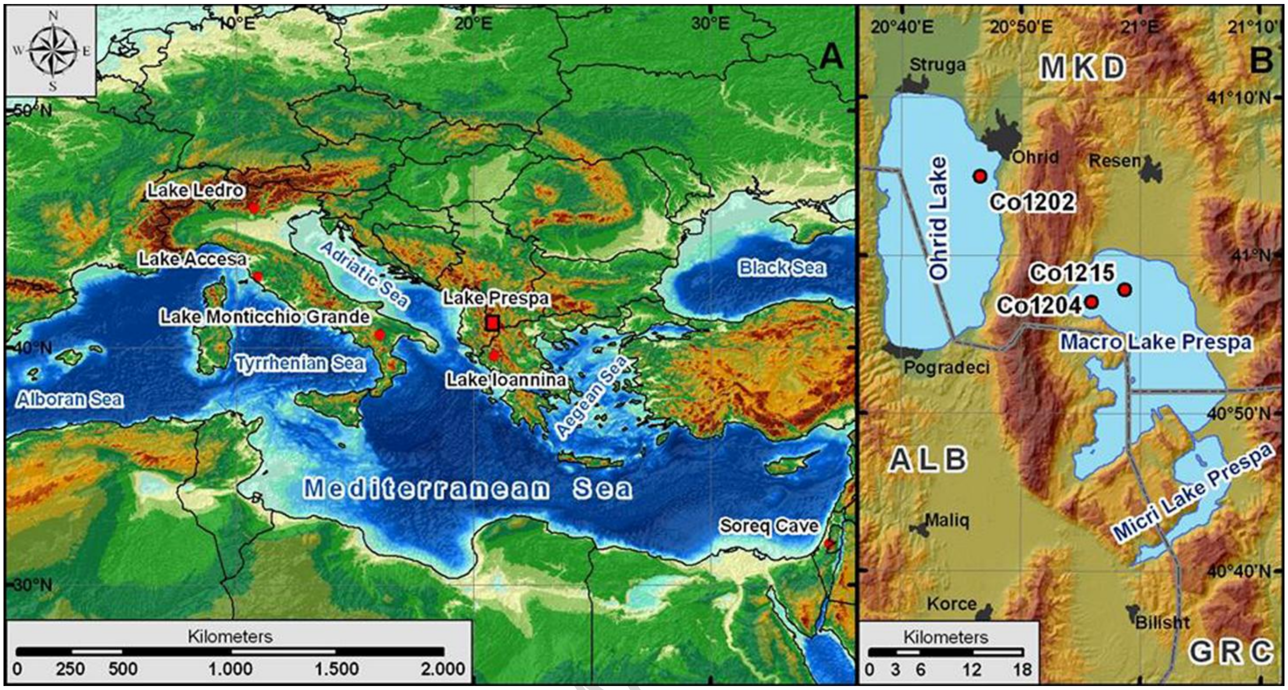
A
N
S
W
E
10°E
20°E
30°E
50°N
40°N
30°N
Lake Ledro
Lake Accesa
Lake Monticchio Grande
Lake Prespa
Lake Ioannina
Adriatic Sea
Tyrrhenian Sea
Alboran Sea
Black Sea
Aegean Sea
Mediterranean Sea
Soreq Cave
Kilometers
0 250 500 1.000 1.500 2.000
B
20°40'E
20°50'E
21°E
21°10'E
41°10'N
41°N
40°50'N
40°40'N
Struga
MKD
Ohrid
Resen
Ohrid Lake
Co1202
Co1215
Co1204
Macro Lake Prespa
Micri Lake Prespa
Pogradeci
ALB
Maliq
Korce
Bilisht
GRC
Kilometers
0 3 6 12 18

Figure 1

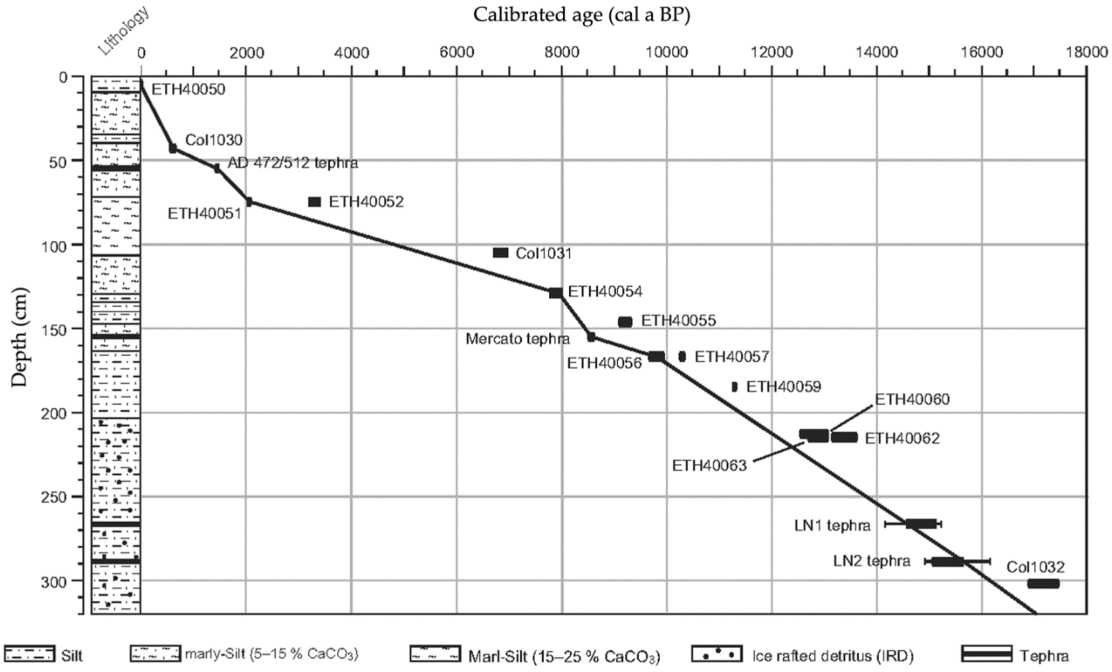
Lithology
Calibrated age (cal a BP)
0
2000
4000
6000
8000
10000
12000
14000
16000
18000
Depth (cm)
0
50
100
150
200
250
300
ETH40050
Col1030
AD 472/512 tephra
ETH40051
ETH40052
Col1031
ETH40054
ETH40055
Mercato tephra
ETH40056
ETH40057
ETH40059
ETH40060
ETH40062
ETH40063
LN1 tephra
LN2 tephra
Col1032
Silt
marly-Silt (5–15 % CaCO₃)
Marl-Silt (15–25 % CaCO₃)
Ice rafted detritus (IRD)
Tephra

Figure 2

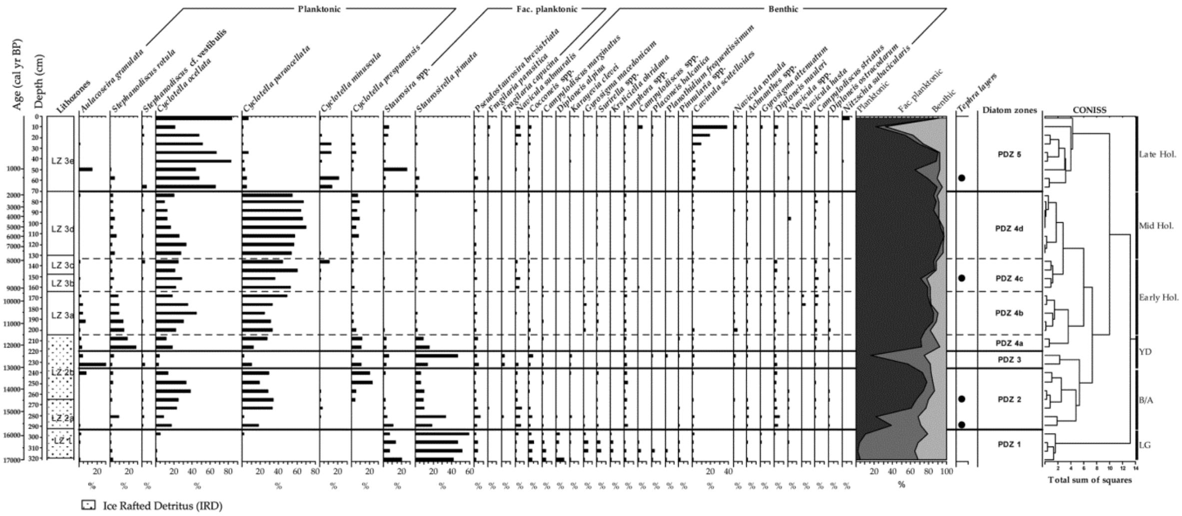
Planktonic
Fac. planktonic
Benthic
Age (cal yr BP)
Depth (cm)
Lithozones
Aulacoseira granulata
Stephanodiscus rotula
Stephanodiscus cf. vestibulis
Cyclotella ocellata
Cyclotella paraocellata
Cyclotella minuscula
Cyclotella prespanensis
Staurosira spp.
Staurosirella pinnata
Pseudostaurosira brevistriata
Fragilaria parasitica
Fragilaria capucina
Navicula submuralis
Cocconeis spp.
Campylodiscus marginatus
Diploneis alpina
Karayevia clevei
Gyrosigma macedonicum
Surirella spp.
Krsticiella ohridana
Amphora spp.
Campylodiscus spp.
Placoneis balcanica
Planothidium frequentissimum
Pinnularia spp.
Cavinula scutelloides
Navicula rotunda
Achnanthes spp.
Gyrosigma attenuatum
Diploneis mauleri
Navicula spp.
Navicula hasta
Campylodiscus striatus
Diploneis ostracodarum
Nitzschia subacicularis
Planktonic
Fac. planktonic
Benthic
Tephra layers
Diatom zones
CONISS
LZ 3e
LZ 3d
LZ 3c
LZ 3b
LZ 3a
LZ 2b
LZ 2a
LZ 1
PDZ 5
PDZ 4d
PDZ 4c
PDZ 4b
PDZ 4a
PDZ 3
PDZ 2
PDZ 1
Late Hol.
Mid Hol.
Early Hol.
YD
B/A
LG
%
Total sum of squares
Ice Rafted Detritus (IRD)

Figure 3

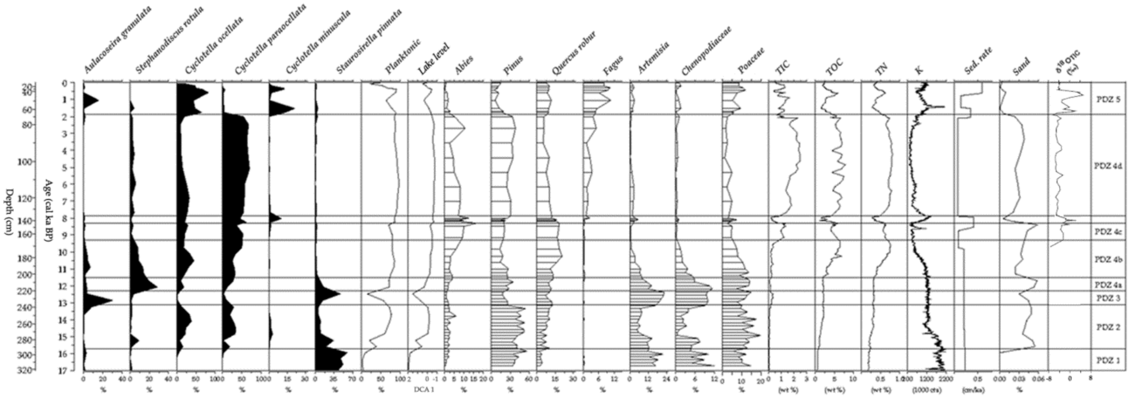
Aulacoseira granulata
Stephanodiscus rotula
Cyclotella ocellata
Cyclotella paraocellata
Cyclotella minuscula
Staurosirella pinnata
Planktonic
Lake level
Abies
Pinus
Quercus robur
Fagus
Artemisia
Chenopodiaceae
Poaceae
TIC
TOC
TN
K
Sed. rate
Sand
δ18OTIC (‰)
Depth (cm)
Age (cal ka BP)
20 40 60 80 100 120 140 160 180 200 220 240 260 280 300 320
0 1 2 3 4 5 6 7 8 9 10 11 12 13 14 15 16 17
%
DCA 1
(wt %)
(1000 cts)
(cm/ka)
PDZ 5
PDZ 4d
PDZ 4c
PDZ 4b
PDZ 4a
PDZ 3
PDZ 2
PDZ 1

Figure 4

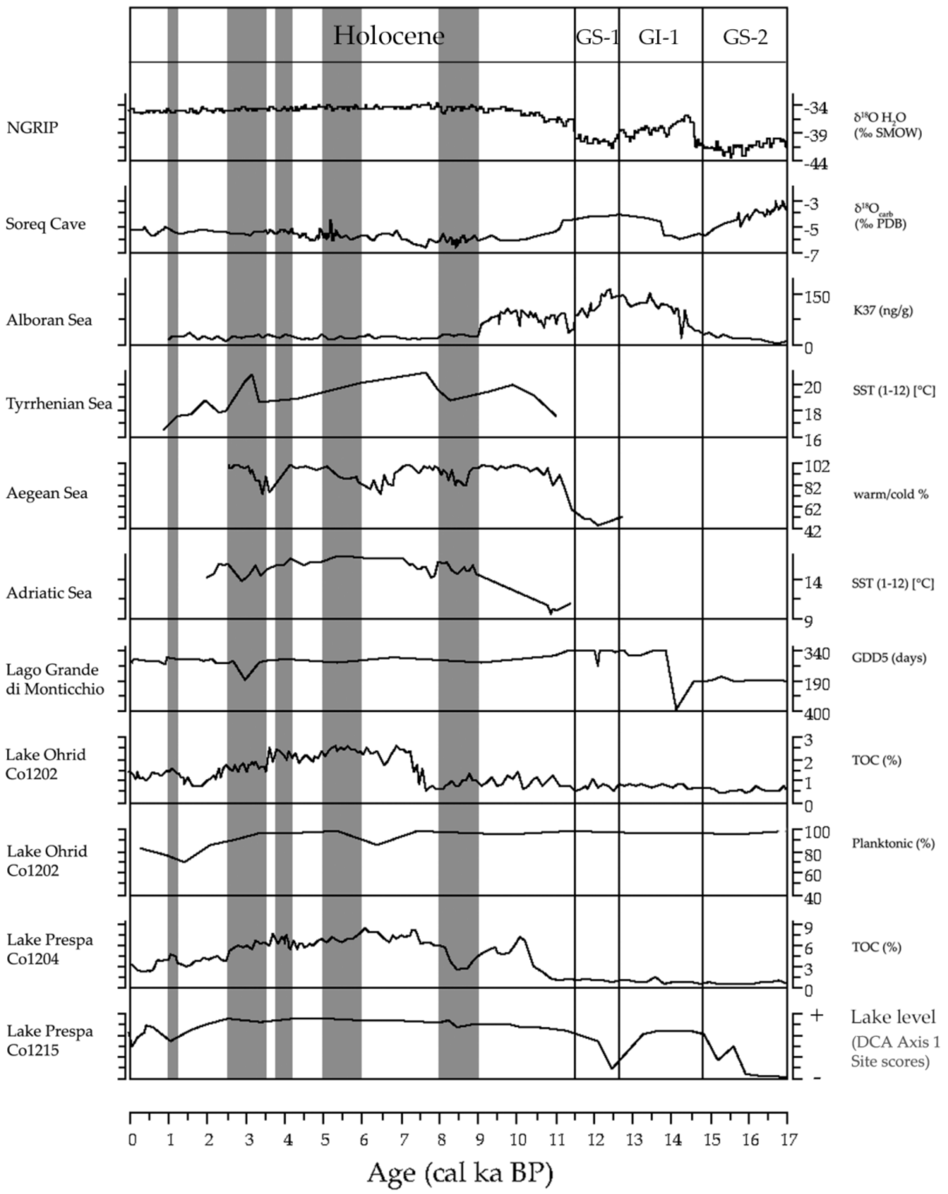
Holocene
GS-1
GI-1
GS-2
NGRIP
-34
-39
-44
δ18O H2O (‰ SMOW)
Soreq Cave
-3
-5
-7
δ18Ocarb (‰ PDB)
Alboran Sea
150
0
K37 (ng/g)
Tyrrhenian Sea
20
18
16
SST (1-12) [°C]
Aegean Sea
102
82
62
42
warm/cold %
Adriatic Sea
14
9
SST (1-12) [°C]
Lago Grande di Monticchio
340
190
400
GDD5 (days)
Lake Ohrid Co1202
3
2
1
0
TOC (%)
Lake Ohrid Co1202
100
80
60
40
Planktonic (%)
Lake Prespa Co1204
9
6
3
0
TOC (%)
Lake Prespa Co1215
+
-
Lake level (DCA Axis 1 Site scores)
0 1 2 3 4 5 6 7 8 9 10 11 12 13 14 15 16 17
Age (cal ka BP)

Figure 5

Fig. 1. Map of the Mediterranean region (A) showing the location of lakes Prespa and Ohrid (red rectangle) and palaeoreconstruction sites used for comparison and referred to in the text: Alboran Sea (Cacho et al. 2002), Tyrrhenian Sea (Cacho et al. 2001), Lago Grande di Monticchio (Allen et al. 1999), Lake Accesa (Magny et al. 2009), Lake Ledro (Magny et al. 2012), Adriatic Sea (Giunta et al. 2001), Lake Ioannina (Wilson et al. 2008), Aegean Sea (Rohling et al. 2002), Soreq Cave (Bar-Matthews et al. 2003). Map of lakes Ohrid and Prespa (B) showing location of core Co1215 and other coring sites referred to in the text: Lake Prespa Co1204 (Wagner et al. 2010) and Lake Ohrid Co1202 (Reed et al. 2010, Vogel et al. 2010, Wagner et al. 2010, Cvetkoska et al. 2012).

Fig.2. Age-depth model with lithology of top 320 cm of core Co1215 (modified from Aufgebauer et al. 2012). Chronological tie points are interpolated on a linear basis.

Fig.3. Stratigraphic diagram of diatom taxa present at >2% abundance in Lake Prespa core Co1215 displaying diatom zones defined with CONISS, lithozones and presence of tephra layers described in Aufgebauer et al. (2012). Explanation of abbreviations: LG (Late Glacial), B/A (Bølling/Allerød interstadial), YD (Younger Dryas), Hol. (Holocene).

Fig.4. Stratigraphic diagram displaying abundance (%) of selected diatom taxa, Planktonic (%) and Lake level curve compared to selected trees and herb pollen percentages (%) (Panagiotopoulos et al. 2013), geochemical proxies, total inorganic carbon (TIC; wt%), total organic carbon (TOC; wt%), total nitrogen (TN; wt%), potassium (K; 1000 cts), Sed. rate (sedimentation rate; cm/ka), sand (%) (Aufgebauer et al. 2012) and $\delta^{18}O_{TIC}$ (‰) (Leng et al. 2013) of Lake Prespa core Co1215. CONISS determined diatom zones are marked. Lake level curve derived from DCA Axis 1 site scores.

Fig.5. Lake-level reconstruction for core Co1215 derived from DCA Axis 1 site scores and total organic carbon (TOC; wt %) of core Co1204 from Lake Prespa (Wagner et al. 2010) compared to diatom plantkon (%) (Cvetkoska et al. 2012) and TOC (wt %) (Vogel et al. 2010) of Co1202 from Lake Ohrid, Lago Grande di Monticchio pollen-based palaeoclimate reconstruction (temperature, annual, sum above 5°C [days] (GDD5)) Allen et al. (1999), Adriatic Sea alkenone-derived sea-surface temperature(SST; Giunta et al. 2001), Aegean Sea SST, based on warm/cold % of planktonic foraminifera (Rohling et al. 2002), Thyrrenian sea alkenone-derived SST (Cacho et al. 2001), Alkenones , C37:3+C37:2 [ng/g] (K37) from sediment core MD95-2043 from the Alboran Sea (Cacho et al. 2002), $\delta^{18}O$ carbonate PDB record from Soreq Cave (Bar-Matthews et al. 2003, data product from Shah et al. 2011) and the NGRIP $\delta^{18}O$ record (Andersen et al. 2006). Explanation: Greenland Stadial GS–2 (17.1–14.8 cal ka BP), Greenland Interstadial GS–1 (14.8–

12.7 cal ka BP), Greenland Stadial GS–1 (12.7–11.5 cal ka BP), Holocene (11.5 cal ka BP–present), gray bands mark Holocene Rapid Climate Change (RCC) events (cf. Mayewski et al. 2004).

Table 1 caption:

Table 1. Results of AMS radiocarbon (^{14}C age [ka BP]) analysis, showing calibrated ages (cal ka BP), for selected plant macrofossils, fish bones, shell remains and bulk sediment samples used to construct the age model for Lake Prespa core Co1215 (modified from Aufgebauer et al. 2012). The radiocarbon ages of all samples were calibrated into calendar years before present using the INTCAL09 calibration curve (Reimer et al., 2009), except for sample ETH-40050 which used the Levin. ^{14}C dataset (Levin and Kromer, 2004).

Sample	Depth (cm)	Material	^{14}C age (ka BP)	Calendar age (cal ka BP [2σ])
ETH-40050	4–6	Shell (*Dreissena presbensis*)	-0.12 ± 0.03	(-0.02) ± 0.00
Col1030	42–44	Plant (*Carex* sp.)	0.72 ± 0.03	0.63 ± 0.06
ETH-40051	74–76	Plant (*Phragmites australis*)	2.08 ± 0.04	2.07 ± 0.08
ETH-40052	74–76	Bulk organic matter	3.09 ± 0.04	3.31 ± 0.07
Col1031	104–108	Bulk organic matter	6.00 ± 0.03	6.84 ± 0.09
ETH-40054	128–130	Bulk organic matter	7.06 ± 0.04	7.89 ±0.07
ETH-40055	146–147	Bulk organic matter	8.21 ± 0.04	9.16 ± 0.13
ETH-40056	166–168	Plant (*Phragmites australis*)	8.76 ± 0.04	9.75 ± 0.15
ETH-40057	166–168	Bulk organic matter	9.09 ± 0.04	10.24 ± 0.05
ETH-40059	184–186	Bulk organic matter	9.84 ± 0.04	11.24 ± 0.04
ETH-40060	212–214	Fish remains	10.84 ± 0.13	12.82 ± 0.26
ETH-40062	214–216	Fish remains	11.47 ± 0.12	13.36 ± 0.25
ETH-40063	214–216	Bulk organic matter	11.01 ± 0.04	12.89 ± 0.19
Col1032	301–303	Plant (aquatic)	14.06 ± 0.07	17.16 ± 0.30

Table 2. Spearman's rho correlation test between *Cyclotella* species and selected geochemical proxies in Lake Prespa core Co1215.

	Cyclotella ocellata		*Cyclotella paraocellata*		*Cyclotella prespanensis*		*Cyclotella minuscula*	
	ρ (rho) coefficient	confidence value (%)	ρ (rho) coefficient	confidence value (%)	ρ (rho) coefficient	confidence value (%)	ρ (rho) coefficient	confidence value (%)
TIC	0.34	32	0.49	84	0.26	47	0.13	9
TOC	0.27	20	0.72	93	0.30	55	-0.03	23
TOC/TN	0.20	12	0.77	96	0.39	61	-0.04	30
K	-0.29	26	-0.71	91	-0.26	52	-0.03	16

Table 3 caption:

Table 3. Summary table of DCA sites scores based on core Co1215 diatom data–eigenvalues, axis length and decorana values of the first four ordination axes.

Axis	**1**	**2**	**3**	**4**
Eigenvalues	0.51	0.30	0.16	0.09
Axis lengths	2.7	1.89	1.71	1.02
Decorana values	0.51	0.26	0.11	0.04

Highlights

- Lake Prespa ca.17 ka diatom sequence generates strong proxy for lake-level changes.
- The diatoms provide evidence for a climatic reversal during the Younger Dryas.
- The diatoms provide clear signal of warm and wet Early Holocene in Lake Prespa.
- The mid Holocene is a period of high lake levels and oligo-mesotrophic conditions.
- The lake-level curve is suggesting a teleconnection with North Atlantic forcing.